ORIGINAL ARTICLE

Study on surface generation in nano-cutting by large-scale molecular dynamics simulation

Feifei Xu [1,2] · Fengzhou Fang [1,3] · Xiaodong Zhang [1]

Abstract

Large-scale molecular dynamics simulations are employed in investigating the nano-cutting process. A cutting tool with 1-μm nose radius and 20-nm edge radius is applied in nano-cutting of silicon with cutting distance attaining 400 nm. The mentioned cutting parameters are relatively larger than those used in the former research studies which would help to obtain the results with relatively high confidence coefficient. The results show that when the UCT is smaller or similar to the stagnation height, the extrusion accompanied with the side flow dominates the material removal mechanism. The generated side flow will deteriorate the generated surface roughness. When cutting at {111}<11-2> direction, bct5-Si phase forms and a part of them is left in the machined subsurface. When cutting at {100}<001> direction, the formed bct5-Si and S-II phases transform to the a-Si phase, when the cutting tool passes through.

Keywords Nano-cutting · Phase transformation · Side flow · Stagnation region · Recovery

1 Introduction

Nano-cutting is a method to manufacture components by using a diamond cutting tool based on an ultra-precision machine tool [1–3]. The generated surface roughness could attain nanometric scale by applying appropriate cutting parameters and cutting tools [4]. However, the diamond cutting tool is not infinitely sharp, which causes the formation of side flow and recovery (SF&R) during and after the action of the cutting tool edge [5]. These two factors will influence the surface roughness and make it deviate from its theoretical value [6–10].

✉ Fengzhou Fang
fzfang@gmail.com

Feifei Xu
yuanfei1116@163.com

Xiaodong Zhang
zhangxd@tju.edu.cn

[1] Institute of Machinery Manufacturing Technology, China Academy of Engineering Physics, Mianyang 621900, China

[2] State Key Laboratory of Precision Measuring Technology & Instruments, Centre of MicroNano Manufacturing Technology, Tianjin University, Tianjin 300072, China

[3] School of Mechanical & Materials Engineering, MNMT-Dublin, University College Dublin, Dublin, Ireland

A useful method, molecular dynamics (MD) simulation [11, 12], has been applied to investigated the influences of the SF&R on surface generation [5]. However, considering the computational efficiency, the parameters used in MD simulation are relatively smaller than those used in practice, such as the cutting distance used in MD is less than 100 nm [5, 13]. The cutting tool edge used is less than 10 nm [5, 14], and the tool nose radius used is less than 50 nm [5, 15]. This, to a certain extent, would influence the confidence coefficient of the simulation results.

Therefore, in this study, 20-nm tool edge and 1-μm tool nose radius have been applied to make the simulation parameters approximate the value used in practice. Besides that, the cutting distance in the simulation attains 400 nm, which is relatively larger than that in the former research studies. Therefore, based on the used simulation parameters, the surface generation and the material removal mechanism in nano-cutting of single crystal silicon could be revealed with a relatively high confidence coefficient.

2 Methods

Figure 1 is the large-scale MD simulation model. In the cutting process, the diamond tool is defined as a rigid body. Blue color is assigned to the interaction region between diamond tool and workpiece, as shown in Figs. 1 and 2. In order to
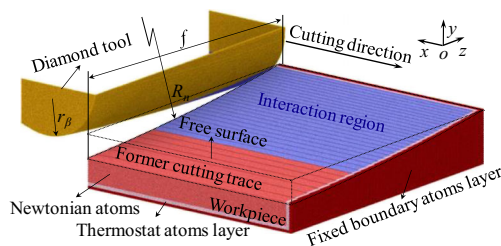
Fig. 1 Nano-cutting model

improve the computational efficiency of the MD simulation model, 1-μm tool nose radius R_n and 20-nm edge radius r_β are used. The values of these two parameters used in this model approximate to those of the cutting tool applied in experiment. The rake and clearance angle used are respectively 0° and 15°. The feed rate f and cutting speed v_c are 126.4 nm/r and 100 m/s. The number of atoms in the workpiece is about 30,000,000, and the size of it is 400 nm × 20 nm × 130 nm. Similar to the former research [5], the former cutting trace is simulated by the cutoff part of the workpiece. Its radius is 1 μm.

In the cutting model, the temperature of the thermostat layer is 293 K and is kept in constant during the cutting process. The Newtonian layer obeys Newton's law. The cutting

distance attains 400 nm, which is relatively longer than that used in the former research studies. The interaction potential and the simulation software used are similar to the former research [5]. The computation time is about 30 days for each program. The software OVITO [16] is also used in analyzing the simulation results.

3 Results and discussion

3.1 Stagnation region and material removal mechanism

Figure 2 is the stagnation region (SR) recognized by the former proposed method [5] at the cutting direction of {100}<001> and {111}<11-2>. When slicing the SR at II-II, III-III, and IV-IV, the SR are shown in Fig. 3b–d and Fig. 4b–d. The materials of the workpiece separate at the tip of the SR. A part of them forms the removed chip and the rest of them forms the machined surface. In Fig. 2, the SR tip is marked with dotted lines. The average vertical distance from the line of the SR tip to the tool edge line AB is the stagnation height (SH).

Fig. 2 SR on the cutting tool edges, at cutting direction of {100}<001> with cutting distance of **a** 36 nm and **b** 400 nm and at cutting direction of {111}<11-2> with cutting distance of **d** 36 nm and **c** 400 nm
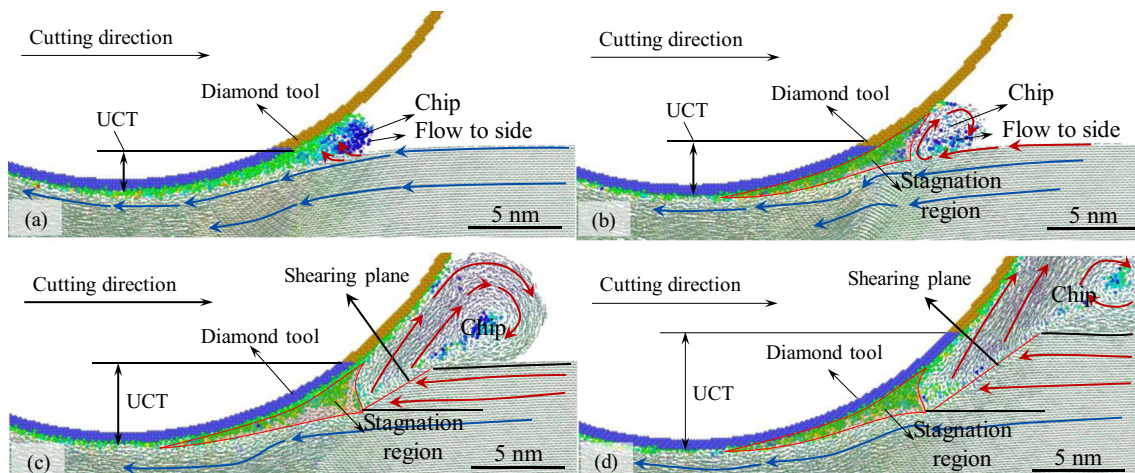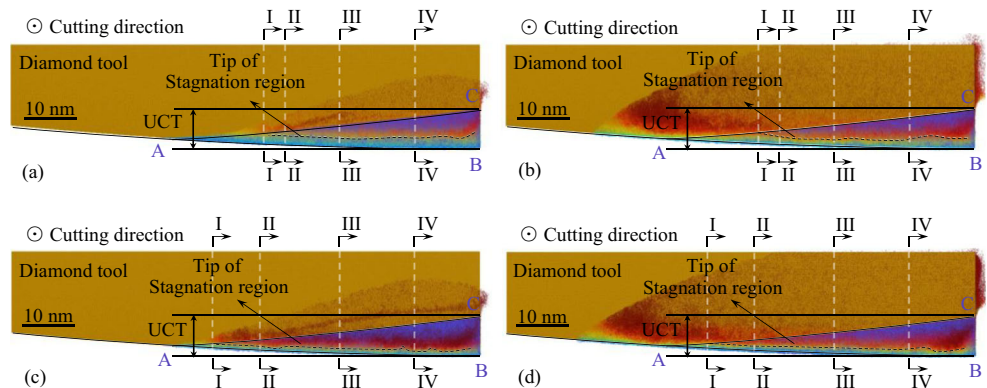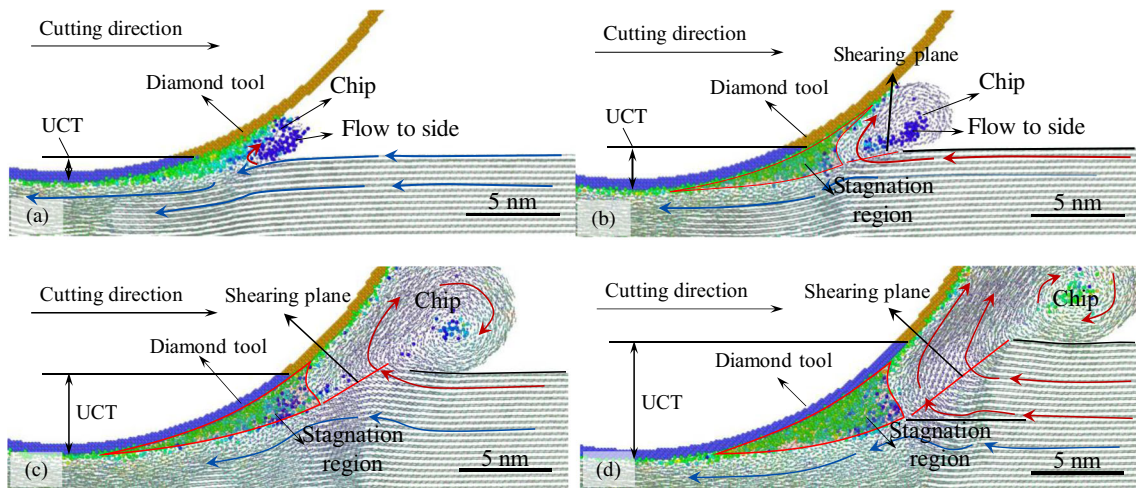

Fig. 3 Displacement vectors sliced in z-direction at **a** I-I, **b** II-II, **c** III-III, and **d** IV-IV, with cutting direction of {100}<001>

Fig. 4 Displacement vectors sliced in *z*-direction at **a** I-I, **b** II-II, **c** III-III, and **d** IV-IV, with cutting direction of {111}<11-2>

As shown in Fig. 2, the SR, including its tip, are located at the interaction region ABC. The vertical distance from line AB to line AC is the uncut chip thickness (UCT). Therefore, from point A to B, the UCT increases gradually from zero to about 8 nm. When the UCT is smaller or similar to the SH, which happens near the intersection point between the line of the SR tip and the line AC, the material is not removed in the traditional shearing mechanism. To further analyze the material removal mechanism in this condition, Figs. 3a and 4a are sliced at the intersection point. The results show that the cutting tool slides on the surface of the workpiece. The upper layer of the workpiece is extruded to form the chip which moves along with the cutting tool. During the cutting process, the extruded chip flows to the side which causes the formation of the SF region. Therefore, along the tool edge, when the UCT is smaller or similar to the SH, the extrusion accompanied with SF dominates the material removal mechanism.

When the UCT is larger than the SH, the material removal phenomena are shown in Figs. 3c, d and 4b–d. These figures are sliced at the place where the line of the stagnation tip is below the line AC. The results show that the displacement

vectors of the atoms change abruptly at a plane that expands from the SR tip. This plane is the shearing plane formed in the nano-cutting process. Therefore, in this condition, due to the formation of SR, materials could be removed by shearing, even when the UCT is relatively smaller than the cutting edge radius.

Comparing Fig. 2 a and b with c and d, the line of the stagnation tip at cutting direction of {111}<11-2> is near the tool edge AB. Therefore, the SH for cutting direction of {111}<11-2> is smaller than that of {100}<001> cutting direction. It implies that more materials in front of the tool edge could be removed by shearing.

3.2 Side flow and recovery

Figure 5 is sliced at *x*-direction and the SF&R regions are displayed. The theoretical surface roughness PV and the SF-influenced surface roughness PV′, which is larger than PV, are also displayed. According to the above section, the material flows to the side when the UCT is smaller or similar to the SH. To clearly reveal the formation mechanism of SF, the displacement vectors of the workpiece atoms are shown in Fig. 6, which are sliced in V-V planes (in Fig. 5) at {100}<001> and {111}<11-2> cutting directions with cutting distances of 36 nm and 360 nm. At the initial cutting stage, when the cutting distance is 36 nm for both cutting directions at Fig. 6a, c, the atoms start to flow to the side at the place where the UCT is smaller or similar to the SH.

In Fig. 6b, d, the cutting distance is 360 nm. A large amount of materials has been extruded and flows to the place where the UCT is about zero. The SF region forms and further causes the increment of the surface roughness. Therefore, with an increase of cutting distance, the amount of the materials which are extruded and form the SF region increases until they attain a stable state. As shown in Fig. 5,
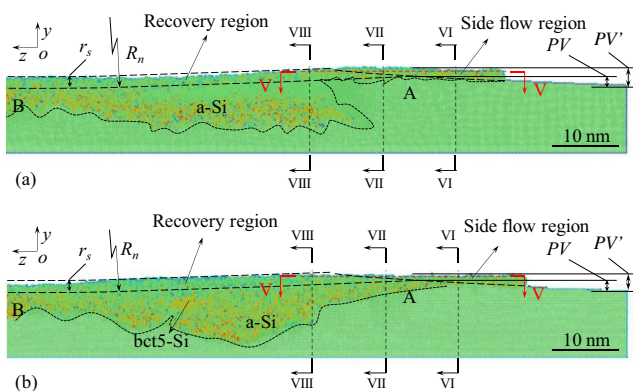

Fig. 5 SF&R region at cutting direction of **a** {100}<001> and **b** {111}<11-2>
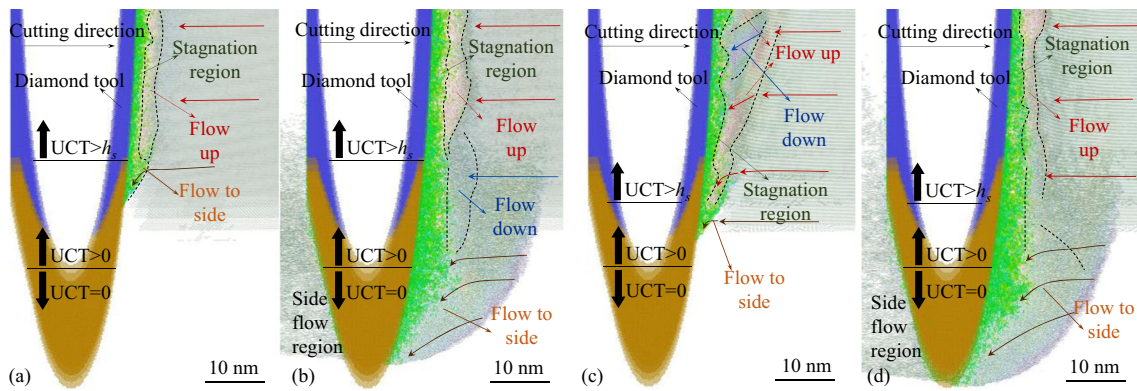
Fig. 6 Displacement vectors sliced in V-V at cutting direction and cutting distance of (**a**) {100}<001>, 36 nm; (**b**) {100}<001>, 360 nm; (**c**) {111}<11-2>, 36 nm; and (**d**) {111}<11-2>, 360 nm

the recovery tends to decrease the SF-influenced surface roughness PV′. And it is almost not affected by the cutting distance.

3.3 Phase transformation

The phase of silicon is analyzed by coordination number (CN). Different phases, such as amorphous phase (a-Si), diamond crystal phase (Si-I), and bct5-Si and β-Sn phase (Si-II), are recognized [17].

At the cutting direction of {100}<001>, the phase transformation is shown in Fig. 7. When the UCT is zero, a lot of materials are extruded and flow down to the machined surface, as shown in Fig. 7a. It makes a thin layer of

amorphous silicon left on the machined surface. This layer also forms the SF region, as shown in Fig. 5a. In Fig. 7b, the UCT is about 1 nm. The silicon transforms from Si-I phase to bct5-Si phase during the cutting process. But after the tool edge cutting passes through, the transformed phase recovers to the Si-I phase, only leaving a layer of a-Si phase in the machined surface. And the thickness of the a-Si layer has slight fluctuation along the cutting direction. When the UCT is larger than 1 nm, the bct5-Si could not recover to Si-I phase, leaving the amorphous phase to penetrate into the subsurface, as shown in Fig. 7c. Si-II phase which is surrounded by the bct5-Si phase also formed during the cutting process. After the tool passes through, the Si-II phase, as well as bct5-Si, transformed to a-Si phase.
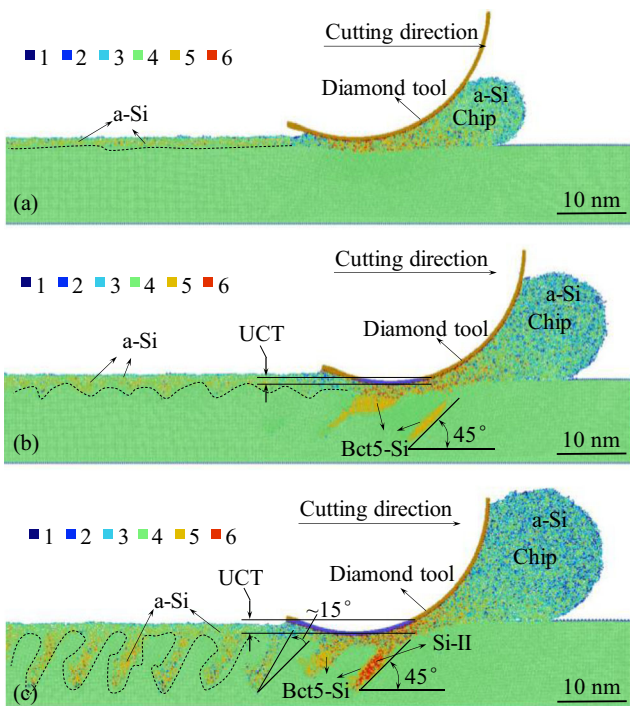

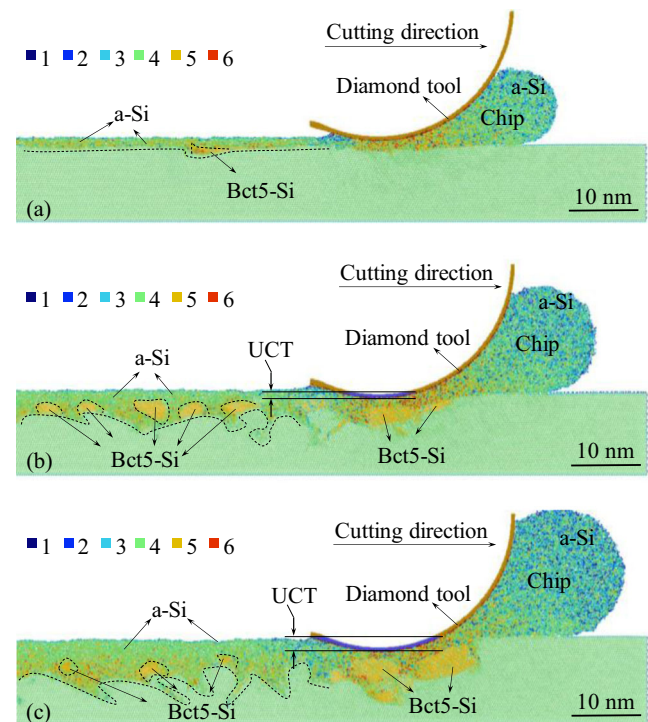**Fig. 7** Phase transformation sliced in **a** VI, **b** VII, and **c** VIII, at cutting direction of {100}<001>

Fig. 8 Phase transformation sliced in **a** VI, **b** VII, and **c** VIII, at cutting direction of {111}<11-2>

Under the cutting edge, the phase transforms at the plane which has a 45° included angle. And after the tool passes through, the phase-transformed plane has a 15° rotation, as displayed in Fig. 7c.

At cutting direction of {111}<11-2>, as shown in Fig. 8, similar to the results obtained at {100}<001> cutting direction, a lot of materials are extruded and flow down to the machined surface forming the a-Si layer and SF region. But there is some difference. Bct5-Si phase forms in the a-Si phase due to the extrusion of the cutting tool, even the UCT is zero (Fig. 8a). When increasing the UCT, bct5-Si phase forms and is surrounded by a-Si phase, as shown in Fig. 8b, c. Therefore, in nano-cutting of silicon at {111}<11-2> direction, bct5-Si phase forms and is left in the machined subsurface. But when cutting at {100}<001> direction, the formed bct5-Si and S-II phases transform to the a-Si phase, when the cutting tool passes through.

4 Conclusions

The large-scale MD simulation model, which has a cutting tool with 1-μm nose radius and 20-nm edge radius and the cutting distance attaining 400 nm, is applied to obtain the simulation results with relatively high confidence coefficient. When the UCT is smaller or similar to the stagnation height, the extrusion accompanied with the side flow dominates the material removal mechanism. The generated side flow will deteriorate the generated surface roughness. When cutting at {111}<11-2> direction, bct5-Si phase forms and a part of them is left in the machined subsurface. When cutting at {100}<001> direction, the formed bct5-Si and S-II phases transform to the a-Si phase, when the cutting tool passes through.

References

1. Xu FF, Fang FZ, Zhang XD (2017) Hard particle effect on surface generation in nano-cutting. Appl Surf Sci 425:1020–1027. https://doi.org/10.1016/j.apsusc.2017.07.089

2. Fang FZ (1998) Nano-turning of single crystal silicon. J Mater Process Technol 82(1–3):95–101. https://doi.org/10.1016/S0924-0136(98)00024-7

3. Fang FZ, Wu H, Liu YC (2005) Modelling and experimental investigation on nanometric cutting of monocrystalline silicon. Int J Mach Tools Manuf 45(15):1681–1686. https://doi.org/10.1016/j.ijmachtools.2005.03.010

4. Fang FZ, Xu FF (2018) Recent advances in micro/nano-cutting: effect of tool edge and material properties. Nanomanuf Metrol 1(1):4–31. https://doi.org/10.1007/s41871-018-0005-z

5. Xu FF, Fang FZ, Zhang XD (2018) Effects of recovery and side flow on surface generation in nano-cutting of single crystal silicon. Comput Mater Sci 143:133–142. https://doi.org/10.1016/j.commatsci.2017.11.002

6. Pekelharing AJ, Gieszen CA (1971) Material side flow in finish turning. Annals of the CIRP 20(1):21–22

7. Grzesik W (1996) A revised model for predicting surface roughness in turning. Wear 194(1):143–148. https://doi.org/10.1016/0043-1648(95)06825-2

8. Liu K, Melkote SN (2006) Effect of plastic side flow on surface roughness in micro-turning process. Int J Mach Tools Manuf 46(14):1778–1785. https://doi.org/10.1016/j.ijmachtools.2005.11.014

9. Zong WJ, Huang YH, Zhang YL, Sun T (2014) Conservation law of surface roughness in single point diamond turning. Int J Mach Tools Manuf 84:58–63. https://doi.org/10.1016/j.ijmachtools.2014.04.006

10. Schaal N, Kuster F, Wegener K (2015) Springback in metal cutting with high cutting speeds. Procedia CIRP 31:24–28

11. Shi J, Wang YC, Yang XP (2013) Nano-scale machining of polycrystalline coppers - effects of grain size and machining parameters. Nanoscale Res Lett 8(1):500. https://doi.org/10.1186/1556-276x-8-500

12. Wang ZG, Chen JX, Wang GL, Bai QS, Liang YC (2017) Anisotropy of single-crystal silicon in nanometric cutting. Nanoscale Res Lett 12(1):300. https://doi.org/10.1186/s11671-017-2046-4

13. Goel S, Martinez FD, Chavoshi SZ, Khatri N, Giusca C (2018) Molecular dynamics simulation of the elliptical vibration-assisted machining of pure iron. J Micromanuf 1(1):6–19. https://doi.org/10.1177/2516598418765359

14. Goel S, Stukowski A, Luo XC, Agrawal A, Robert LR (2013) Anisotropy of single-crystal 3C–SiC during nanometric cutting. Model Simul Mater Sci Eng 21(6):065004

15. Lai M, Zhang XD, Fang FZ, Bi MH (2017) Fundamental investigation on partially overlapped nano-cutting of monocrystalline germanium. Precis Eng 49:160–168. https://doi.org/10.1016/j.precisioneng.2017.02.004

16. Alexander S (2010) Visualization and analysis of atomistic simulation data with OVITO–the open visualization tool. Model Simul Mater Sci Eng 18(1):015012

17. Kim DE, Oh SI (2006) Atomistic simulation of structural phase transformations in monocrystalline silicon induced by nanoindentation. Nanotechnology 17(9):2259–2265